



Cite this: *Phys. Chem. Chem. Phys.*,
2020, 22, 11567

Strain induced spin-splitting and half-metallicity in antiferromagnetic bilayer silicene under bending

Jin-Lei Shi,^{†a} Yunhua Wang,^{†ab} Xing-Ju Zhao,^c Yu-Zhong Zhang,^d
Shengjun Yuan,^{be} Su-Huai Wei^{*a} and Dong-Bo Zhang^{*ac}

Searching for half-metals in low dimensional materials is not only of scientific importance, but also has important implications for the realization of spintronic devices on a small scale. In this work, we show theoretically that simple bending can induce spin-splitting in bilayer silicene. For bilayer silicene with Bernal stacking, the monolayer has a long range ferromagnetic spin order and between the two monolayers, the spin orders are opposite, giving rise to an antiferromagnetic configuration for the ground state of the bilayer silicene. Under bending, the antiferromagnetic spin order is retained but the energetic degeneracy of opposite spin states is lifted. Due to the unusual deformation potentials of the conduction band minimum (CBM) and valence band maximum (VBM) as revealed by density-functional theory calculations and density-functional tight-binding calculations, this spin-splitting is nearly proportional to the degree of bending deformation. Consequently, the spin-splitting can be significant and the desired half-metallic state may emerge when the bending increases, which has been verified by direct simulation of the bent bilayer silicene using the generalized Bloch theorem. Our results hint that bilayer silicene may be an excellent candidate for half-metallicity.

Received 10th March 2020,
Accepted 24th April 2020

DOI: 10.1039/d0cp01350a

rsc.li/pccp

Introduction

The pursuit of half-metals (HMs) represents a fundamental task in stimulating scientific research and actual applications of spintronics.^{1,2} Although several bulk HM systems have been experimentally identified such as ferromagnetic manganese perovskite,³ Heusler compounds^{4–6} and oxides,⁷ HMs in two dimensions (2D) have not been realized yet.

Due to its novel physical properties, graphene has been considered as a promising candidate in the realization of long-awaited 2D spintronics.^{8,9} Partially, this is because graphene is naturally compatible with the current technologies using main group semiconductors. Also, the weak spin-orbit coupling allows for a long relaxation time, a property useful for the performance

of spintronics. As pioneered by the Louie group,¹⁰ the realization of HMs has been predicted to be possible in zigzag graphene nanoribbons (ZGNRs) by applying a transverse electric field. Later, it was shown that an equivalent transverse electric field over the GNRs can be induced *via* chemical decorations.^{11–14} However, these proposals encounter difficulties associated with their experimental realization. The successfully synthesized graphene/hexagonal boron nitrogen (hBN) lateral heterostructures where a zigzag GNR is sandwiched by hBN NRs provide an alternative route to access the HM states.^{15,16} Unfortunately the obtained HM is substantially suppressed. Moreover, strain engineering of 2D materials has been widely used in recent theoretical and experimental efforts^{17–19} to induce novel states. Representative examples include strain tailored magnetic properties and valley splitting in layered 2H-VSe₂¹⁷ and 2H-VS₂/Cr₂C heterostructures,¹⁸ as well as the pronounced HM character in bent ZGNRs.¹⁹ So far, seeking HM systems in 2D is still under active investigation.

Silicene is isoelectronic to graphene and exhibits several fascinating properties, such as the quantum spin Hall effect,²⁰ quantum anomalous Hall and valley polarized quantum Hall effect,²¹ and giant magnetoresistance,²² inviting extensive theoretical and experimental investigation.^{20,23–26} Monolayer silicene has been successfully synthesised on diverse substrates.^{23–25} Recently, few-layer silicene was also obtained experimentally,^{25,27–30} with

^a Beijing Computational Science Research Center, Beijing, 100193, P. R. China.

E-mail: suhuaiwei@csrc.ac.cn, dbzhang@bnu.edu.cn

^b Institute for Molecules and Materials, Radboud University, Heijendaalseweg 135, NL-6525, AJ, Nijmegen, The Netherlands

^c College of Nuclear Science and Technology, Beijing Normal University, Beijing 100875, P. R. China

^d Shanghai Key Laboratory of Special Artificial Microstructure Materials and Technology, School of Physics Science and Engineering, Tongji University, Shanghai 200092, P. R. China

^e Key Laboratory of Artificial Micro- and Nano-structures of Ministry of Education and School of Physics and Technology, Wuhan University, Wuhan, 430072, China

† Contributed equally.

intriguing properties beyond the monolayer, such as chiral superconductivity,³¹ magnetic quantization behaviors,³² and topological³³ and optoelectronic properties.³⁴ In particular, by virtue of its intrinsic magnetism and spontaneous band gap opening,³⁵ bilayer silicene is of great potential for application in spintronics and nanoelectronic devices.^{21,36} For example, it was recently reported that the HM can be induced in bilayer silicene by applying external electric fields and with extra electron doping.³⁷

In this work, we show that spin-splitting can be induced in bilayer silicene by an out-of-plane bending without applying electric fields. Note that such bending deformation is quite viable for 2D materials. Such spin-splitting originates from the unusual deformation potential of the electronic states. Using first-principles calculations, we revealed that for AB-stacking bilayer silicene with an antiferromagnetic order, the deformation potential is negative for both conduction band minimum (CBM) and valence band maximum (VBM). In this way, the spin-splitting will be enlarged if the bending deformation increases and the half-metallic states can be obtained.

Methods

All the density functional theory (DFT) calculations³⁸ are performed by using the VASP code,³⁹ Kohn–Sham equations are solved using the projector-augmented-wave (PAW) method⁴⁰ with a plane-wave basis set and periodic boundary conditions. Exchange correlation energy is calculated using the Perdew–Burke–Ernzerhof functional.⁴¹ The effect of van de Waals (vdW) interactions is taken into account by using the empirical correction scheme of Grimme.⁴² For all studied structures, an energy cutoff of 500 eV is used and the Brillouin-zone sampling is performed on $31 \times 31 \times 1 \kappa$ mesh determined by the Monkhorst–Pack scheme. Vacuum slabs of 25 Å thickness are used to obtain two-dimensional models.

For the bent bilayer silicene, see Fig. 2, because the translational symmetry is removed, standard electronic structure calculation approaches are not applicable any longer. The direct simulation of bilayer silicene under pure bending is enabled by the generalized Bloch theorem coupled with self-consistent charge density-functional tight-binding (SCC-DFTB),^{19,43} where the rotational symmetry is used to depict the electronic states. In this approach, the bent bilayer silicene is described with repetition rules of translation \mathbf{T} , and rotations \mathbf{R} of angle Ω are performed around the bending axis on the N atoms cell (note that here $N = 8$),

$$\mathbf{X}_{j,\zeta_1,\zeta_2} = \mathbf{R}^{\zeta_1} \mathbf{X}_j + \zeta_2 \mathbf{T}, \quad j = 1, \dots, N. \quad (1)$$

where, \mathbf{X}_j represents atoms inside the primitive repeating cell and $\mathbf{X}_{j,\zeta_1,\zeta_2}$ represents the atoms inside the replica of the repeating cell indexed by (ζ_1, ζ_2) . The bending angle Ω of the rotational matrix \mathbf{R} satisfies $\lambda_1 \Omega = 2\pi$ with λ_1 being an integer number and $\zeta_1 = 0, 1, \dots, \lambda_1 - 1$. $\zeta_2 = 0, 1, \dots, \lambda_2 - 1$ where $\lambda_2 \rightarrow \infty$.

The generalized Bloch theorem is formulated as,

$$\psi_{j,\alpha}(k, \mathbf{r}) = \frac{1}{\sqrt{\lambda_1 \lambda_2}} \sum_{\zeta_1 \zeta_2} \exp(ik\zeta_1 + ik\zeta_2) \mathbf{R}^{\zeta_1} \mathbf{T}^{\zeta_2} \varphi_{j,\alpha}(\mathbf{r}), \quad (2)$$

where, $\varphi_{j,\alpha}(\mathbf{r})$ refers to the atomic orbital α on atom j . α runs over all the orbitals of a single atom and j runs over all the $N = 8$ atoms inside the primitive cell. The phase factors are the eigenvalues of rotation and translation. Quantum number $0 \leq \kappa < 2\pi$ adopts values in integral multiples of Ω .

Additionally, to build the bended bilayer silicene model, we need to get the optimal unit cell of bilayer silicene, and then according to the bending angle Ω , the radii R_0 of the bended structure can be determined by $R_0 = a_0/(\Omega * \pi/180)$, where a_0 is the lattice constant of bilayer silicene. Furthermore, based on the initial coordinates of the unit cell of bilayer silicene, the bended unit cell of bilayer silicene can be obtained by rotation matrix \mathbf{R} according to the known R_0 and bending angle Ω .

The generalized Bloch theorem has been implemented^{19,43} in the computational package dftb⁴⁴ by us. In our SCC-DFTB calculations, for the bilayer silicene under pure bending, a series of bending angles Ω are considered. 100 κ points are used to converge the band energy. The collinear treatment for atomic spin is adopted.

Results and discussion

The bilayer silicene discussed in the present work is shown in Fig. 1(a) and (b) with an AB-stacking pattern.^{30–32,34,35} For this structure, it has an electronic ground state with the antiferromagnetic (AFM) spin order. Thus, although the bilayer silicene is metallic without considering the spin freedom, Fig. 1(d), a band gap is opened when the super exchange interaction of long-range spin order is involved in the electronic structure calculations, Fig. 1(e). Fig. 1(c) shows the spin density distribution of the

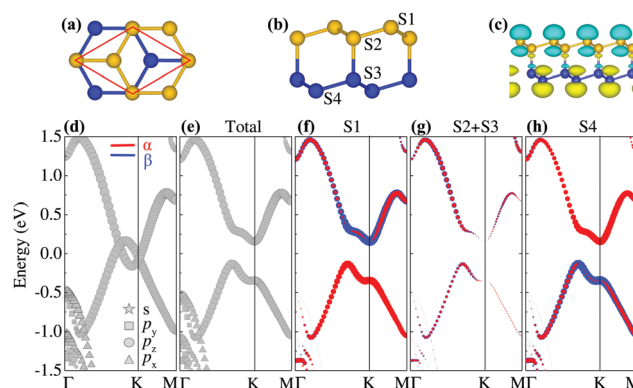


Fig. 1 Local structure of top (a) and side (b) view of an AB-stacking bilayer silicene. For distinction, the yellow and blue balls refer to the upper and lower layer Si atoms, respectively, and the atoms are labeled by S1, S2, S3 and S4. S1 and S2 are in the upper layer while S3 and S4 are in the lower layer. (c) Side view of the calculated spin density ($\rho_\alpha - \rho_\beta$) of bilayer silicene. The spin-up density is in cyan while the spin-down density is in yellow, and the isosurfaces are plotted at 0.20 electrons per Å³; (d and e) are the total orbital-projected structures of nonmagnetic and antiferromagnetic bilayer silicene; (f–h) are the p_z orbitals contributed from the Si atom at the S1 site, the sum of the S2 and S3 site Si atoms (S2 + S3) and the Si atom at the S4 site, respectively. The radii of the circles are proportional to the weights of corresponding orbitals. α and β refer to the spin-up and spin-down states that are shown in red and blue, respectively. The Fermi level is set to zero.

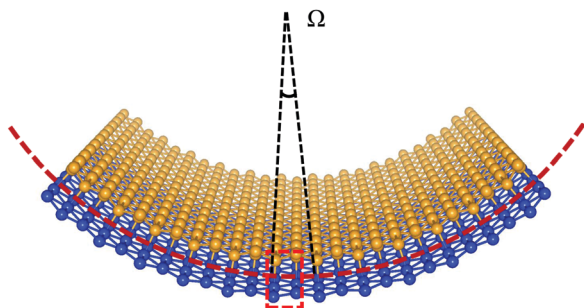


Fig. 2 Bending AB-stacking silicene bilayer. The red dashed rectangle denotes the computational cell. The bending angle corresponding to the computational cell is Ω . For distinction, the yellow and blue balls refer to Si atoms in the different layers.

antiferromagnetic state³⁵ for VBM. The AFM state of the AB-stacking bilayer silicene has a D_{3d} symmetry. The obtained band gap is sizeable, about 0.283 eV in our first-principle calculations, in good agreement with recent reports.⁴⁵

With this, we now explore the strain impact on the AFM state. The deformation exerted to the bilayer is indicated in the inset of Fig. 3(f). The calculated band structures of the bilayer silicene under different strains (ϵ) are shown in Fig. 3(a–c). Note that when plotting the band structure, the electronic energy levels are calibrated with respect to the vacuum level. Usually, in calculations of the absolute deformation potential of 2D materials,

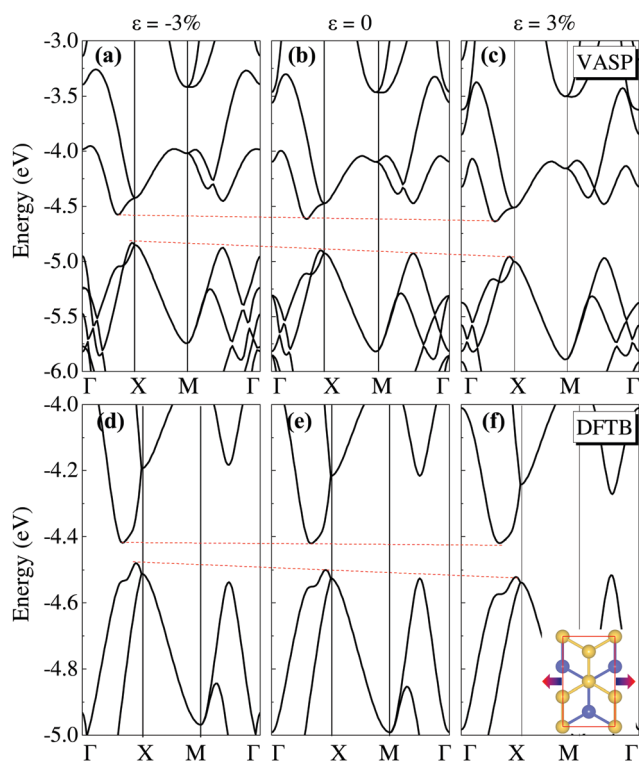


Fig. 3 Electronic band structures of bilayer silicene calculated by DFT under different axial strains: (a) compressive strain $\epsilon = -3\%$, (b) stress-free $\epsilon = 0\%$, (c) tensile strain $\epsilon = 3\%$. (d–f) The corresponding results calculated using the SCC-DFTB method. The vacuum energy is used as the reference. The inset picture is the unit cell and the arrow is the strain direction.

the vacuum level is widely used as the energy reference to align the band structure.⁴⁶ We focus on the behavior of band edges of CBM and VBM. We can see that as ϵ increases (*i.e.*, from compression to tension), both CBM and VBM adopt downward shifts, and the variation of CBM is much less than that of VBM. These behaviors give rise to an increase of the band gap of the bilayer and more importantly, indicate that both the CBM and VBM are of negative deformation potentials. This is quite odd for a typical covalent system. In general, for conventional covalent semiconductors,^{47,48} volume deformation potential of the CBM (a_v^{CBM}), which is the antibonding state of cation s and anion s orbitals, is negative. That is, the CBM state moves upward in energy when the system is under pressure due to the increase in the kinetic energy and the s - s level repulsion. On the other hand, the volume deformation potential of the VBM state (a_v^{VBM}), which is mostly determined by the kinetic energy and p - p coupling effects, is usually positive. That is, the energy level for the VBM state generally decreases as the volume decreases.

In order to understand the obtained unusual deformation potential, we explore the detailed electronic properties of bilayer silicene. From Fig. 1(d) and (e), we see that both CBM and VBM states consist of the component of p_z orbitals. Thus, it is reasonable to obtain similar behaviors of CBM and VBM in response to strains. Fig. 1(f)–(h) give the p_z orbital-projected band structure of bilayer silicene. It can be seen that these states reside on S1 and S4 atoms with the minor part on S2 and S3 atoms. Therefore, the in-plane bonding between p_z orbitals is rather weak and the response of such states to strain is essentially dominated by the variation in the kinetic energy of the electrons.¹⁹ This explains the sign of the deformation potentials of VBM and CBM.

Furthermore, one can also see that these electronic states are spin polarized. In accordance with the AFM configuration, the spin orientations of the VBM state on S1 and S4 are opposite and so are the spin orientations of the CBM state. Notice that S1 and S4 are in different layers, as shown in Fig. 1(c), indicating a spatial separation of spin states.

Also, we have verified the unusual deformation potentials using the SCC-DFTB method. As shown in Fig. 3(d)–(f), we can see that the SCC-DFTB results reveal similar behaviors of CBM and VBM states when strain is applied. The energy levels of both CBM and VBM states shift upwards under compression, in good agreement with the DFT calculations.

With the unusual deformation potential of CBM and VBM, and the revealed spatial separation of spin charge in bilayer silicene, it is possible to induce spin-splitting by inhomogeneous strains. We consider an out-of-plane bending deformation. The results calculated by using the generalized Bloch theorem are summarized in Fig. 4, with pure bending angles at $\Omega = 0.0^\circ, 1.0^\circ, 3.0^\circ, 5.0^\circ$ and 6.0° , respectively. As expected, the spin-splitting at the CBM and VBM states of bilayer silicene appear under pure bending, and as the bending angle Ω becomes larger, the splitting magnitude becomes more significant. For the bending angle at 6.0° , the gap between the spin-down states is nearly closed, indicating that the HM state may be approached. Notice that around $k = \pi$, there are valence states that move up rapidly upon bending, Fig. 4(b)–(e).

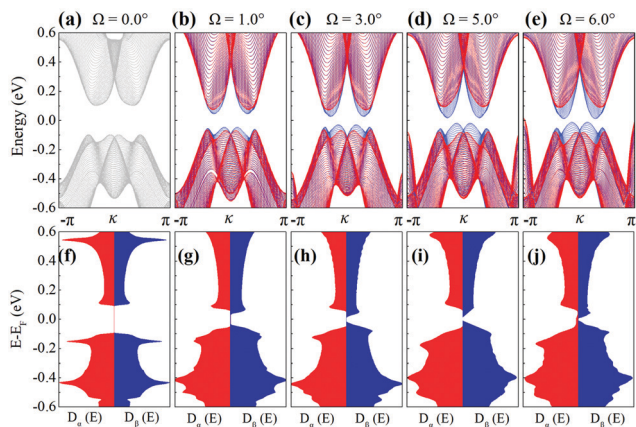


Fig. 4 Spin-resolved electronic band structures and the density-of-states of the AB-stacking silicene bilayer under different pure bending angles (Ω): (a) $\Omega = 0.0^\circ$, (b) $\Omega = 1.0^\circ$, (c) $\Omega = 3.0^\circ$, (d) $\Omega = 5.0^\circ$ and (e) $\Omega = 6.0^\circ$, respectively. The red and blue solid lines denote bands of spin-up states and spin-down states, respectively. The lower panels (f–j) are the corresponding density of states, the electronic states on the left (red) and right (blue) are the spin-up and spin-down states, respectively.

This is because these states have a much greater deformation potential than that of VBM states. According to Fig. 1(d) and (e), we see that these states are composed of mainly an s orbital and p_x and p_y orbitals. Thus, the bonding of these states is within the monolayer and covalent-type. Nonetheless, we note that their impact on the HM feature is not significant, because their density of states near the Fermi level is small.

For a practically useful HM system, it is also important to explore the stability of the long-range magnetic order. The stability of a magnetic order can be quantitatively characterized by the energy difference between the AFM and nonmagnetic (NM) states.¹⁰ To verify the magnetic stability, we calculate the energy difference between the AFM and NM states in bilayer silicene under pure bending as follows:

$$\Delta E = E_{\text{NM}} - E_{\text{AFM}}, \quad (3)$$

Here, E_{AFM} and E_{NM} denote the energies of the AFM and NM states, respectively. Results are shown in Fig. 5. For a stress free silicene bilayer ($\Omega = 0.0^\circ$), ΔE is indeed large, which is about

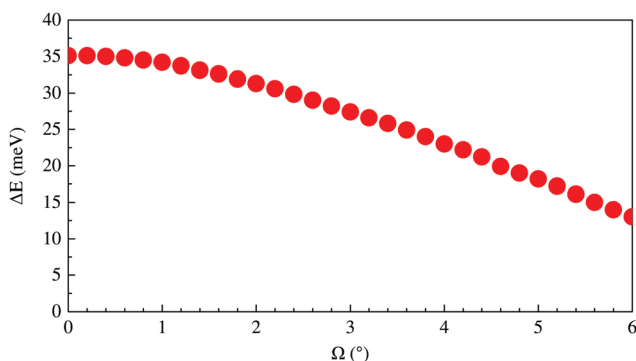


Fig. 5 Dependence of magnetic interaction energy ΔE per unit cell on bending angle Ω , for bilayer silicene.

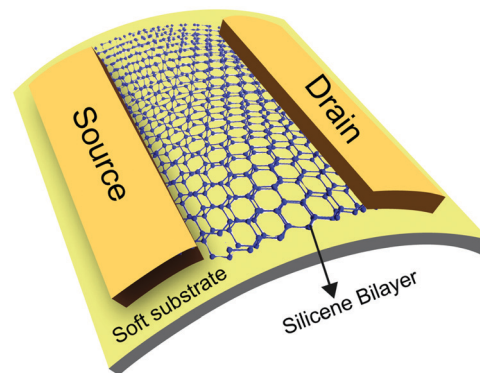


Fig. 6 Schematic diagram of a possible spin filter or spin generator device generated by using a silicene bilayer placed on a certain flexible substrate. The bending is posed through the soft substrate.

35.1 meV per unit cell. Under bending, the magnetic stability of ΔE is slightly decreasing as the bending angle Ω is increasing; even at a bending angle of $\Omega = 6.0^\circ$, ΔE is around 14 meV per unit cell, suggesting that the magnetic stability of the bilayer silicene with pure bending is well retained in the effective spin-splitting bending range.

Based on the above results, we furthermore propose that a possible spin filter or a spin generator device can be designed by a bent silicene bilayer on certain flexible substrates, as shown in Fig. 6. For the maintenance of the well retained AFM states of an AB-stacking silicene bilayer, strong electronic interaction between silicene monolayers and the substrate should be avoided. In view of this, we also suggest that certain polymer insulators such as polyethylene terephthalate film and poly-methyl methacrylate can be used, which can stabilize the silicene bilayers essentially through non-electronic van der Waals interactions.⁴⁹

Conclusions

In conclusion, we propose a new mechanism for inducing spin-splitting in bilayer silicene through strain engineering. Combining first-principles calculations and generalized Bloch theorem, we revealed the unusual deformation potential in bilayer silicene. The degenerate CBM and VBM spin-states can be easily lifted by introducing an inhomogeneous strain through the out-of-plane bending. Note that such a bending deformation is quite common for layered systems of only few-atom thickness. The gap-closure of one of the spin-polarized states can be achieved at a large bending angle, indicating that it is possible to realize half-metallicity in such a system. Furthermore, we also notice that the magnetic stability of the long range magnetic order for the antiferromagnetic states is retained well against the bending deformation. These aspects indicate that bilayer silicene is a promising material for the realization of half-metallicity in low dimensions.

Conflicts of interest

There are no conflicts to declare.

Acknowledgements

This work was supported by the Ministry of Science and Technology of China under Grant No. 2017YFA0303400, the National Natural Science Foundation of China (NSFC) under Grant Nos 11674022, 51672023, 11634003 and No. U1930402. D.-B. Z. was supported by the Fundamental Research Funds for the Central Universities. Computations were carried out at the Beijing Computational Science Research Center.

Notes and references

- C. Felser, G. Fecher and B. Balke, *Angew. Chem., Int. Ed.*, 2007, **46**, 668–699.
- D. D. Awschalom and M. E. Flatté, *Nat. Phys.*, 2007, **3**, 668–699.
- J.-H. Park, E. Vescovo, H.-J. Kim, C. Kwon, R. Ramesh and T. Venkatesan, *Nature*, 1998, **392**, 794–796.
- R. A. de Groot, F. M. Mueller, P. G. V. Engen and K. H. J. Buschow, *Phys. Rev. Lett.*, 1983, **50**, 2024–2027.
- M. Jourdan, J. Minár, J. Braun, A. Kronenberg, S. Chadov, B. Balke, A. Gloskovskii, M. Kolbe, H. Elmers and G. Schönhense, *Nat. Commun.*, 2014, **5**, 3974.
- K. E. H. M. Hanssen, P. E. Mijnders, L. P. L. M. Rabou and K. H. J. Buschow, *Phys. Rev. B: Condens. Matter Mater. Phys.*, 1990, **42**, 1533–1540.
- Y. Ji, G. J. Strijkers, F. Y. Yang, C. L. Chien, J. M. Byers, A. Anguelouch, G. Xiao and A. Gupta, *Phys. Rev. Lett.*, 2001, **86**, 5585–5588.
- W. Han, R. K. Kawakami, M. Gmitra and J. Fabian, *Nat. Nanotechnol.*, 2014, **9**, 794–807.
- D. Pesin and A. H. MacDonald, *Nat. Mater.*, 2012, **11**, 409–416.
- Y. W. Son, M. L. Cohen and S. G. Louie, *Nature*, 2006, **444**, 347.
- O. Hod, V. Barone, J. E. Peralta and G. E. Scuseria, *Nano Lett.*, 2007, **7**, 2295–2299.
- D. Gunlycke, J. Li, J. W. Mintmire and C. T. White, *Appl. Phys. Lett.*, 2007, **91**, 112108.
- M. Wu, X. Wu, Y. Gao and X. C. Zeng, *Appl. Phys. Lett.*, 2009, **94**, 223111.
- E.-j. Kan, Z. Li, J. Yang and J. G. Hou, *J. Am. Chem. Soc.*, 2008, **130**, 4224–4225.
- J. M. Pruneda, *Phys. Rev. B: Condens. Matter Mater. Phys.*, 2010, **81**, 161409.
- D. Zhang, D.-B. Zhang, F. Yang, H.-Q. Lin, H. Xu and K. Chang, *2D Mater.*, 2015, **2**, 041001.
- S. Feng and W. Mi, *Appl. Surf. Sci.*, 2018, **458**, 191–197.
- X. Ma, L. Yin, J. Zou, W. Mi and X. Wang, *J. Phys. Chem. C*, 2019, **123**, 17440–17448.
- D. B. Zhang and S. H. Wei, *npj Comput. Mater.*, 2017, **3**, 32.
- C.-C. Liu, W. Feng and Y. Yao, *Phys. Rev. Lett.*, 2011, **107**, 076802.
- M. Ezawa, *Phys. Rev. Lett.*, 2012, **109**, 055502.
- C. Xu, G. Luo, Q. Liu, J. Zheng, Z. Zhang, S. Nagase, Z. Gao and J. Lu, *Nanoscale*, 2012, **4**, 3111–3117.
- B. Feng, Z. Ding, S. Meng, Y. Yao, X. He, P. Cheng, L. Chen and K. Wu, *Nano Lett.*, 2012, **12**, 3507–3511.
- P. Vogt, P. De Padova, C. Quaresima, J. Avila, E. Frantzeskakis, M. C. Asensio, A. Resta, B. Ealet and G. Le Lay, *Phys. Rev. Lett.*, 2012, **108**, 155501.
- L. Tao, E. Cinquanta, D. Chiappe, C. Grazianetti, M. Fanciulli, M. Dubey, A. Molle and D. Akinwande, *Nat. Nanotechnol.*, 2015, **10**, 227.
- S. Cahangirov, M. Topsakal, E. Aktürk, H. S. Sahin and S. Ciraci, *Phys. Rev. Lett.*, 2009, **102**, 236804.
- R. Yaokawa, T. Ohsuna, T. Morishita, Y. Hayasaka, M. J. S. Spencer and H. Nakano, *Nat. Commun.*, 2016, **7**, 10657.
- P. De Padova, O. Kubo, B. Olivieri, C. Quaresima, T. Nakayama, M. Aono and G. Le Lay, *Nano Lett.*, 2012, **12**, 5500–5503.
- Z.-X. Guo and A. Oshiyama, *Phys. Rev. B: Condens. Matter Mater. Phys.*, 2014, **89**, 155418.
- A. Popescu, P. Rodriguez-Lopez and L. M. Woods, *Phys. Rev. Mater.*, 2019, **3**, 064002.
- F. Liu, C.-C. Liu, K. Wu, F. Yang and Y. Yao, *Phys. Rev. Lett.*, 2013, **111**, 066804.
- T.-N. Do, P.-H. Shih, G. Gumbs, D. Huang, C.-W. Chiu and M.-F. Lin, *Phys. Rev. B*, 2018, **97**, 125416.
- M.-M. Zhang, L. Xu and J. Zhang, *J. Phys.: Condens. Matter*, 2015, **27**, 445301.
- B. Huang, H.-X. Deng, H. Lee, M. Yoon, B. G. Sumpter, F. Liu, S. C. Smith and S.-H. Wei, *Phys. Rev. X*, 2014, **4**, 021029.
- X. Wang and Z. Wu, *Phys. Chem. Chem. Phys.*, 2017, **19**, 2148–2152.
- Z. Ni, Q. Liu, K. Tang, J. Zheng, J. Zhou, R. Qin, Z. Gao, D. Yu and J. Lu, *Nano Lett.*, 2012, **12**, 113–118.
- X.-F. Ouyang, Z.-Y. Song and Y.-Z. Zhang, *Phys. Rev. B*, 2018, **98**, 075435.
- P. Hohenberg and W. Kohn, *Phys. Rev.*, 1964, **136**, B864–B871.
- G. Kresse and J. Hafner, *Phys. Rev. B: Condens. Matter Mater. Phys.*, 1993, **47**, 558–561.
- P. E. Blöchl, *Phys. Rev. B: Condens. Matter Mater. Phys.*, 1994, **50**, 17953–17979.
- J. P. Perdew, K. Burke and M. Ernzerhof, *Phys. Rev. Lett.*, 1996, **77**, 3865–3868.
- S. Grimme, *J. Comput. Chem.*, 2006, **27**, 1787–1799.
- L. Yue, G. Seifert, K. Chang and D.-B. Zhang, *Phys. Rev. B*, 2017, **96**, 201403.
- B. Aradi, B. Hourahine and T. Frauenheim, *J. Phys. Chem. A*, 2007, **111**, 5678–5684.
- X. Wang and Z. Wu, *Phys. Chem. Chem. Phys.*, 2017, **19**, 2148–2152.
- J. Wiktor and A. Pasquarello, *Phys. Rev. B*, 2016, **94**, 245411.
- S.-H. Wei and A. Zunger, *Phys. Rev. B: Condens. Matter Mater. Phys.*, 1999, **60**, 5404–5411.
- Y.-H. Li, X. G. Gong and S.-H. Wei, *Phys. Rev. B: Condens. Matter Mater. Phys.*, 2006, **73**, 245206.
- G. Tsoukleri, J. Parthenios, K. Papagelis, R. Jalil, A. C. Ferrari, A. K. Geim, K. S. Novoselov and C. Galiotis, *Small*, 2009, **5**, 2397–2402.